Ocean Sci., 19, 941–952, 2023
https://doi.org/10.5194/os-19-941-2023

Ocean Science Open Access EGU

Dense water formation in the eastern Mediterranean under a global warming scenario

Iván M. Parras-Berrocal[1], Rubén Vázquez[1,2], William Cabos[2], Dimitry V. Sein[3,4], Oscar Álvarez[1], Miguel Bruno[1], and Alfredo Izquierdo[1]

[1]Instituto Universitario de Investigación Marina (INMAR), Universidad de Cádiz, Puerto Real, Cádiz 11510, Spain
[2]Department of Physics and Mathematics, University of Alcalá, Alcalá de Henares 28801, Spain
[3]Alfred Wegener Institute for Polar and Marine Research, 27570 Bremerhaven, Germany
[4]Shirshov Institute of Oceanology, Russian Academy of Science, Moscow 117997, Russia

Correspondence: Iván M. Parras-Berrocal (ivan.parras@uca.es)

Received: 3 February 2023 – Discussion started: 16 February 2023
Revised: 22 May 2023 – Accepted: 24 May 2023 – Published: 28 June 2023

Abstract. Dense water formation in the eastern Mediterranean (EMed) is essential in sustaining the Mediterranean overturning circulation. Changes in the sources of dense water in the EMed point to changes in the circulation and water properties of the Mediterranean Sea. Here we examine with a regional climate system model the changes in the dense water formation in the EMed through the 21st century under the RCP8.5 emission scenario. Our results show a shift in the dominant source of Eastern Mediterranean Deep Water (EMDW) from the Adriatic Sea to the Aegean Sea in the first half of the 21st century. The projected dense water formation is reduced by 75 % for the Adriatic Sea, 84 % for the Aegean Sea, and 83 % for the Levantine Sea by the end of the century. The reduction in the intensity of deep water formation is related to hydrographic changes in surface and intermediate water that strengthen the vertical stratification, hampering vertical mixing and thus convection. Those changes have an impact on the water that flows through the Strait of Sicily to the western Mediterranean and therefore on the whole Mediterranean system.

1 Introduction

The eastern Mediterranean Sea (EMed) is a key region where intermediate and deep water convection is regularly observed, leading to a vertical recirculation (Roether et al., 1996), which is essential in sustaining the Mediterranean thermohaline circulation (MTHC). Atlantic Water (AW) flows through the Strait of Gibraltar, compensating for the Mediterranean Sea freshwater deficit (Bethoux and Gentili, 1999; Sanchez-Gomez et al., 2011), getting denser through its path to the EMed. Intermediate water in the Levantine Sea is formed by wintertime air–sea interactions that cool the AW, increasing its density and originating Levantine Intermediate Water (LIW; LIWEX group, 2003; Millot et al., 2014). LIW spreads westward at intermediate depths (150–600 m) and then to the Atlantic Ocean, driving the main thermohaline circulation cell of the Mediterranean (Lascaratos et al., 1993; Millot, 2019). Along its path through the eastern and western Mediterranean, the warmer and saltier LIW preconditions the surface waters for deep water formation (DWF) in regions such as the Gulf of Lions, the Adriatic Sea, and the Aegean Sea during the winter months (MEDOC Group, 1970).

The Adriatic Sea has been identified as the main source of Eastern Mediterranean Deep Water (EMDW), as it fills the EMed deep layers (Pollack, 1951; Malanotte-Rizzoli et al., 1997). In winter, the Adriatic DWF is triggered by (i) the cold and dry bora winds (north-easterly), which induce large surface buoyancy loss as a result of a rapid surface cooling and strong evaporation (Lascaratos et al., 1999), and (ii) the presence of LIW, which favours the deepening of the convective layer (Mantziafou and Lascaratos, 2008). Here, most of the DWF takes place in southern Adriatic through open convection inside the Southern Adriatic Pit depression where it is strongly preconditioned by the presence of a permanent cyclonic gyre (Lascaratos et al., 1999; Manca

et al., 2002; Mantziafou and Lascaratos, 2008). Moreover, a smaller amount of deep water is also formed on the continental shelf of the northern and middle Adriatic. During the 1990s, hydrographic surveys showed that the EMDW was mostly formed in the Aegean Sea, inducing the so-called Eastern Mediterranean Transient (EMT; Roether et al., 1996). The main mechanisms leading to the DWF in the Aegean Sea are open-sea convection due to the cooling of surface water, the preconditioning of cyclonic circulation, and the basin salinity increase (Nittis et al., 2003). The main formation sites are the Cyclades plateau, the Syros–Chios basins, and the Creta Sea. Nittis et al. (2003) point out that the annual DWF rate for the Aegean Sea (0.24 Sv) during the EMT was comparable to the 0.3 Sv formed each year in the Adriatic Sea for the 1979–1994 period. Consequently, the Adriatic Sea and the Aegean Sea compete to be the dominant source of DWF in the EMed (Roether et al., 2014). The leading role depends on the water density conditions reached during winter months (Klein et al., 2000).

According to projections of future climate, the Mediterranean Sea has been identified as one of the most responsive regions to climate change. By the end of the 21st century the IPCC scenarios project a warmer and drier Mediterranean climate (Ali et al., 2022). The sea surface temperature (SST) is expected to increase from 0.5 to 3.7 °C, while intermediate and deep layers warm by 0.8–3.0 and 0.15–0.18 °C, respectively (Somot et al., 2006, 2008; Adloff et al., 2015; Darmaraki et al., 2019; Parras-Berrocal et al., 2020; Soto-Navarro et al., 2020; Ali et al., 2022). These changes under global warming may impact the main mechanisms leading to DWF and the MTHC. A recent study has analysed the future response of the main spots for DWF in the Mediterranean to climate change in downscaled climate simulations, pointing to a reduction of deep convection in all regions (Soto-Navarro et al., 2020). In fact, the DWF in the north-western Mediterranean is projected to collapse by the mid-21st century due to the increases in the vertical density gradient between surface and intermediate waters, which strengths the stratification in the water column, hampering deep convection (Parras-Berrocal et al., 2022).

The dense (intermediate and deep) water formation in the EMed has been extensively studied (e.g. Roether et al., 1996; Lascaratos et al., 1999; Nittis et al., 2003; Mantziafou and Lascaratos, 2008; Androulidakis et al., 2012; Dunic et al., 2018; Li and Tanhua, 2020). A lot of attention has also been focused on the causes of the EMT and its impacts, especially on the Mediterranean circulation (e.g. Roether et al., 1996, 2014; Borzelli et al., 2009; Beuvier et al., 2010; Incarbona et al., 2016). However, the response of the EMed dense water formation to climate change has only been briefly assessed by Somot et al. (2006), Adloff et al. (2015), and Soto-Navarro et al. (2020), so a detailed analysis about the expected changes and their causes is needed. Thus, the aim of this work is to study the impact of climate change on the dense water formation in the EMed (Adriatic, Aegean, and Levantine seas, Fig. 1) by the end of the century, as well as to identify the mechanisms involved in those changes. To address this issue we use a regional climate system model (RCSM), which has been widely employed to analyse the present and future climate of the Mediterranean Sea (Darmaraki et al., 2019; Parras-Berrocal et al., 2020; de la Vara et al., 2022), including the interannual variability of DWF in the north-western Mediterranean (Parras-Berrocal et al., 2022).

The paper is organized as follows: in Sect. 2 the RCSM and the simulations employed in this work are described. In Sect. 3, the present climate and future evolution of intermediate and deep water formation in the EMed are analysed. Finally, the discussion of the results and the conclusions are contained in Sect. 4.

2 RCSM setup and simulations

In this work we use the RCSM ROM (ROM) (REMO-OASIS-MPIOM; Sein et al., 2015). In ROM, the regional atmosphere model REMO (Jacob, 2001) is coupled to the global oceanic model MPIOM (Max Planck Institute Ocean Model; Jungclaus et al., 2013; Marsland et al., 2003) via the OASIS3 coupler (Valcke, 2013). ROM also comprises other sub-models such as the HAMburg Ocean Carbon Cycle model (Maier-Reimer et al., 2005), the Hydrological Discharge model (Hagemann and Dümenil-Gates, 1998, 2001), a soil model (Rechid and Jacob, 2006), and a dynamic–thermodynamic sea ice model (Hibler, 1979), which are treated as modules of either the atmosphere or the ocean.

REMO is formulated on a rotated grid with the centre of the domain situated around the Equator in the rotated coordinates with a constant horizontal resolution of 25 km and a total of 27 hybrid levels. The atmospheric domain used in this study extends to the North Atlantic, the eastern tropical Pacific, and the Mediterranean Sea (de la Vara et al., 2022; Vazquez et al., 2022). MPIOM has an orthogonal curvilinear grid with a variable horizontal resolution ranging from 7 km at the southern Alboran Sea to 25 km on the eastern coasts of the Levantine Sea (Fig. 1a). The horizontal resolution in the Adriatic and the Aegean seas is not coarser than 16 and 19 km, respectively. On the vertical, the model has 40 z levels with increasing layer thickness with depth, from 16 m at the surface to 550 m near the seafloor (Parras-Berrocal et al., 2020). Contrary to other RCSMs developed to analyse the Mediterranean Sea, the water exchange at Gibraltar is not parameterized and the properties of the Atlantic waters are not relaxed toward climatological values. In fact, the water exchange through the Strait of Gibraltar is explicitly reproduced, which allows the North Atlantic signal to propagate into the Mediterranean Sea and vice versa. The spin-up of MPIOM was performed according to Sein et al. (2015). First, MPIOM runs in stand-alone mode starting with climatological temperature and salinity data (Levitus et al., 1998). Afterwards, it is integrated four times through the 1958–2002

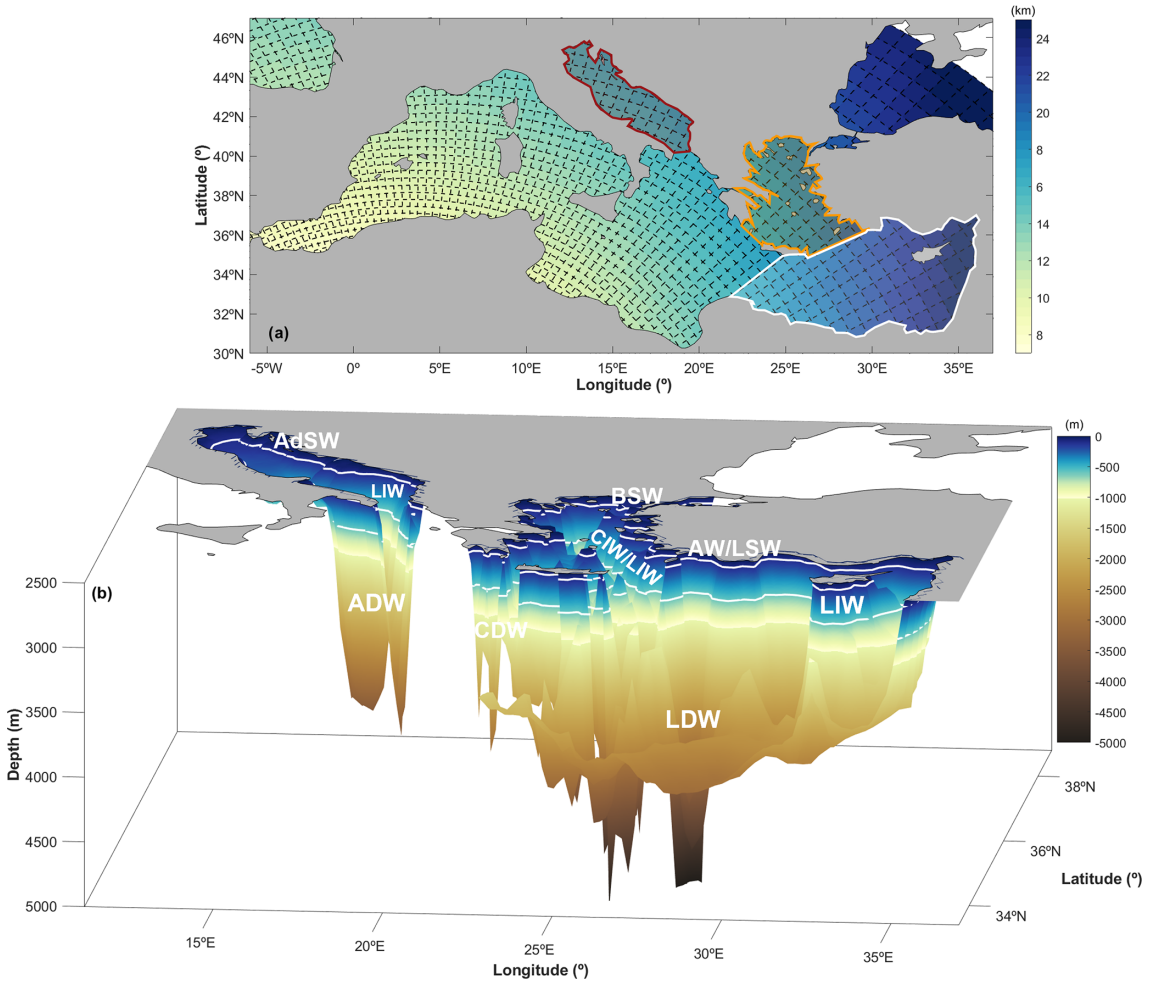

Figure 1. **(a)** Oceanic computational grid and resolution adopted in ROM (in kilometres; only one out of four lines is drawn). The domains used for the calculations in each sub-basin are surrounded by colour lines: Adriatic (red), Aegean (orange), and Levantine (grey). **(b)** Bathymetry of the main spots for dense water formation in the EMed: Adriatic Sea, Aegean Sea, and Levantine Sea. The main water masses of each spot sorted by depth range are also shown: [0–100 m] Adriatic Surface Water (AdSW), Black Sea Water (BSW), Levantine Surface Water (LSW), [100–650 m] Levantine Intermediate Water (LIW), Cretan Intermediate Water (CIW), [650–1000 m] Adriatic Deep Water (ADW), Cretan Deep Water (CDW), and Levantine Deep Water (LDW).

period forced by ERA40. For the coupled runs, the model starts from the final state reached in the last stand-alone run and integrated again, forced two times by ERA40 and one time by ERA-Interim reanalysis (1979–2012). Then, it runs for 56 years (1950–2005) starting from the last state of the coupled simulation forced by ERA-Interim. More information about the model parameterization and setup, as well as a detailed evaluation of Mediterranean present climate and future changes simulated by ROM, can be found in Parras-Berrocal et al. (2020).

To assess the ROM performance in reproducing the dense water formation in the EMed, we use a simulation forced by ERA-Interim (1980–2012), which has been previously defined as ROM_P0 in Parras-Berrocal et al. (2020, 2022). In order to study the interannual variability of dense water formation in the EMed during the present and future climate we take the data from the 1976 to 2005 period of the historical run (ROM_P1) and from 2006 to 2099 of the climate change projection under the RCP8.5 scenario (ROM_P2). All simulations employed in this work are part of the MedCORDEX initiative (https://www.medcordex.eu, last access: 19 January 2023). The domains used for the calculations in each sub-basin are shown in Fig. 1a.

3 Results

3.1 Present-day EMed deep water convection

In this section, we evaluate the ROM_P0 skills in reproducing the average rate and the interannual variability of DWF in the EMed during the present climate (1980–2012). To quan-

tify the DWF over the Adriatic, Aegean, and Levantine seas we have computed the annual DWF rate for a specific isopycnic surface (σ_θ). The DWF rate is calculated from the difference between the maximum volume of water denser than σ_θ for a given year minus the minimum volume of that water for the previous year (Somot et al., 2018). According to Somot et al., (2018), following the volume of the deep water for a given σ_θ (denser than σ_θ) is the best quantitative way to study the DWF in a model output.

The interannual DWF rate in the Adriatic Sea (Fig. 2a) agrees well ($r = 0.70$ at 95 % confidence level, p value $= 0.001$) with estimates based on the Princeton Ocean Model (POM) of Mantziafou and Lascaratos (2008). ROM_P0 (POM) shows annual rates ranging from 0.01 (0.12) Sv to 0.50 (0.93) Sv. During 1981–1999, ROM_P0 produces 5.45 Sv yr of new waters denser than 29.0 kg m^{-3}, corresponding to an annual formation rate of 0.29 Sv (Fig. 2a), which is comparable to the 0.3 Sv estimated by Roether and Schlitzer (1991) from tracer data. Mantziafou and Lascaratos (2008) simulated 7.51 Sv yr of total volume of deep water ($\sigma > 29.1$ kg m^{-3}), corresponding to an annual rate of 0.40 Sv, which overestimates the mean annual rate of Roether and Schlitzer (1991). On the other hand, the interannual DWF rate in the Aegean Sea (Fig. 2b) is also well correlated ($r = 0.75$, p value $= 0.002$) with the POM results reported by Nittis et al. (2003). The total volume of deep water formed during 1981–1994 by ROM_P0 ($\sigma > 28.95$ kg m^{-3}) corresponds to an annual formation rate of 0.30 Sv. This is close to values presented in Nittis et al. (2003), where the total volume formed in the same period is 3.62 Sv yr ($\sigma > 29.2$ kg m^{-3}), leading to an annual rate of 0.26 Sv (Fig. 2b).

ROM_P0 has demonstrated a good performance simulating the average and interannual DWF rate in the Adriatic and Aegean seas. However, the potential density of the newly formed waters in ROM_P0 is lower than those presented by observations (Fig. S1 in the Supplement) and other models. We find that the potential densities of ROM_P0 at 650 m depth are 0.1 and 0.2 kg m^{-3} lighter than WOA18 (Boyer et al., 2018) for the Adriatic and Aegean (Fig. S1), respectively. The deep water generated in the Adriatic Sea has densities between 29.1 and 29.25 kg m^{-3} (Schlitzer et al., 1991; Gačić et al., 2002; Mantziafou and Lascaratos, 2008), while in the Aegean Sea it is denser than 29.2 kg m^{-3} (Klein et al., 1999; Nittis et al., 2003; Beuvier et al., 2010). In ROM_P0 the DWF takes place at $\sigma > 29.0$ kg m^{-3} for the Adriatic Sea and at $\sigma > 28.95$ kg m^{-3} for the Aegean (Fig. 2).

In the Levantine basin, for ROM_P0, the total volume of intermediate and deep water ($\sigma > 28.7$ kg m^{-3}) formed during the period 1981–2012 is 22.3 Sv yr, which corresponds to a mean yearly production of 0.69 Sv. This amount of water produced in the Levantine Sea agrees very well with the 0.69 Sv suggested by Lascaratos et al. (1993), calculated for water denser than 28.92 kg m^{-3} with a mixed layer model. The formation rate simulated by ROM_P0 is consistent with previous estimates that range between 0.6 and 1.3 Sv (Ovchinnikov, 1984; Tziperman and Speer, 1994; Lascaratos et al., 1999). In addition to the Adriatic and Aegean Sea, the potential density simulated by ROM_P0 at 300 m depth in the Levantine Sea is 0.15 kg m^{-3} lighter than WOA18 (Fig. S1). The potential density of the intermediate and deep water formed in the Levantine Sea by ROM_P0 $\sigma > 28.7$ kg m^{-3} is lower than the $\sigma > 28.85$ kg m^{-3} defined by Lascaratos et al. (1993). Despite the lighter densities, we have identified the isopycnals in which the DWF occurs in ROM_P0 for the studied areas. This allows us to assess the projected climate change signal in the EMed DWF under the RCP8.5 scenario with the aim of contributing to the Med-CORDEX initiative to generate useful climatic information.

3.2 Impact of climate change on dense water formation in the EMed

We now examine the yearly evolution of the DWF rate in the 21st century over the main spots for dense water formation in the EMed. To achieve this aim, we have computed the DWF rate for the isopycnals that we have identified in the previous section as the isopycnals where the DWF takes place in the ROM. Thus, we have used 29.0 kg m^{-3} as a lower density bound for the Adriatic Sea, 28.95 kg m^{-3} for the Aegean Sea, and 28.7 kg m^{-3} for the Levantine Sea.

In the Adriatic, Aegean, and Levantine seas the averaged DWF rates for 1976–2005 are 0.32 ± 0.09, 0.25 ± 0.22, and 0.80 ± 0.30 Sv, while for 2070–2099 under RCP8.5 they are 0.08 ± 0.04, 0.04 ± 0.02, and 0.14 ± 0.18 Sv (Fig. 3a, b, and c), respectively. The DWF rate is expected to decrease by 75 % in the Adriatic, 84 % in the Aegean, and almost 83 % in Levantine Sea for the 2070–2099 period compared to 1976–2005. The results suggest that the reduction of dense water formation in the three studied regions starts by the mid-21st century under the RCP8.5 scenario; the nonparametric change-point Pettitt test (Pettit, 1979; Table S1 in the Supplement) detects abrupt changes in DWF rates by 2054 in the Adriatic and Levantine seas ($K = 2.9$, p value $= 0$), while in the Aegean the shift happens by 2040 ($K = 2.5$, p value $= 0$). During the 2005–2040 period the total volume of deep water formed in the Aegean Sea (13.4 Sv yr) is higher than in the Adriatic (9.93 Sv yr) (Fig. 3a, b), which means a shift in the dominant source of EMDW.

In order to identify the mechanisms leading to the projected reduction of dense water formation in the EMed, we have evaluated (i) the role of the winter air–sea fluxes through the accumulated surface buoyancy loss (BL) and (ii) the stratification index (SI). The BL (Eq. 2) was computed as the time integral of the buoyancy flux (BF, Eq. 1) for every year (Y) of the 1976–2099 period from December of the previous year (T_1) to March (T_2) and averaged over the Adriatic, Aegean, and Levantine basins. The BF is calculated as the sum of contributions of heat and freshwater fluxes (Marshall and Schott,

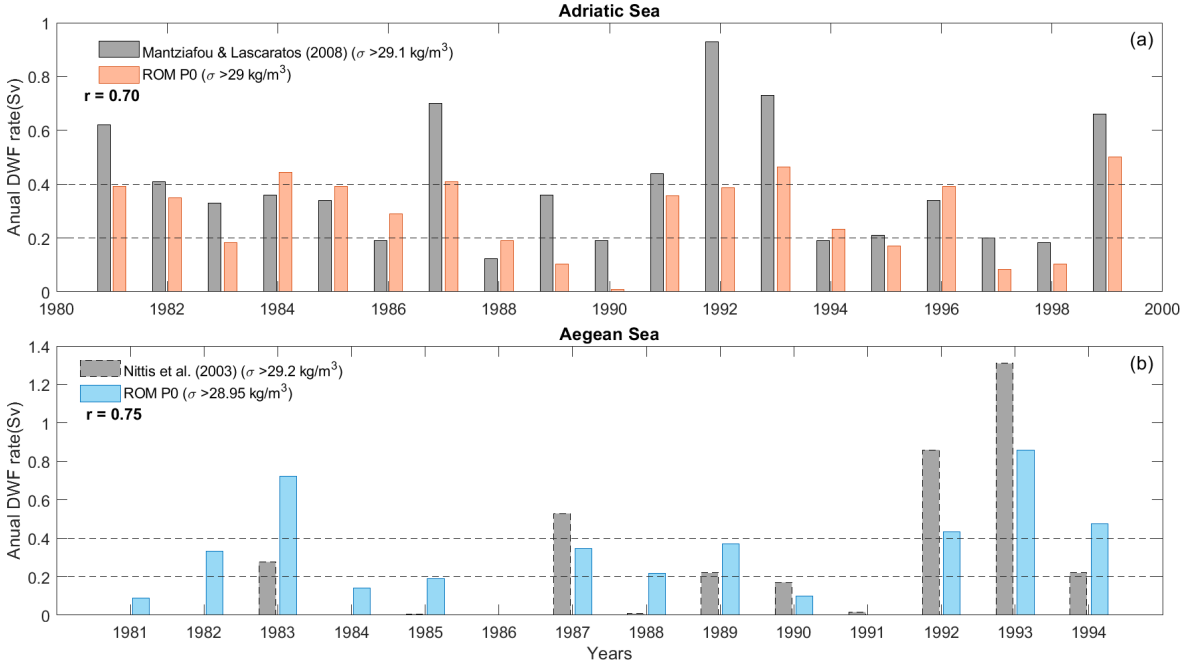

Figure 2. Annual formation rate (Sv) of deep water in the **(a)** Adriatic Sea and **(b)** Aegean Sea. Note the different ranges on vertical and horizontal axes.

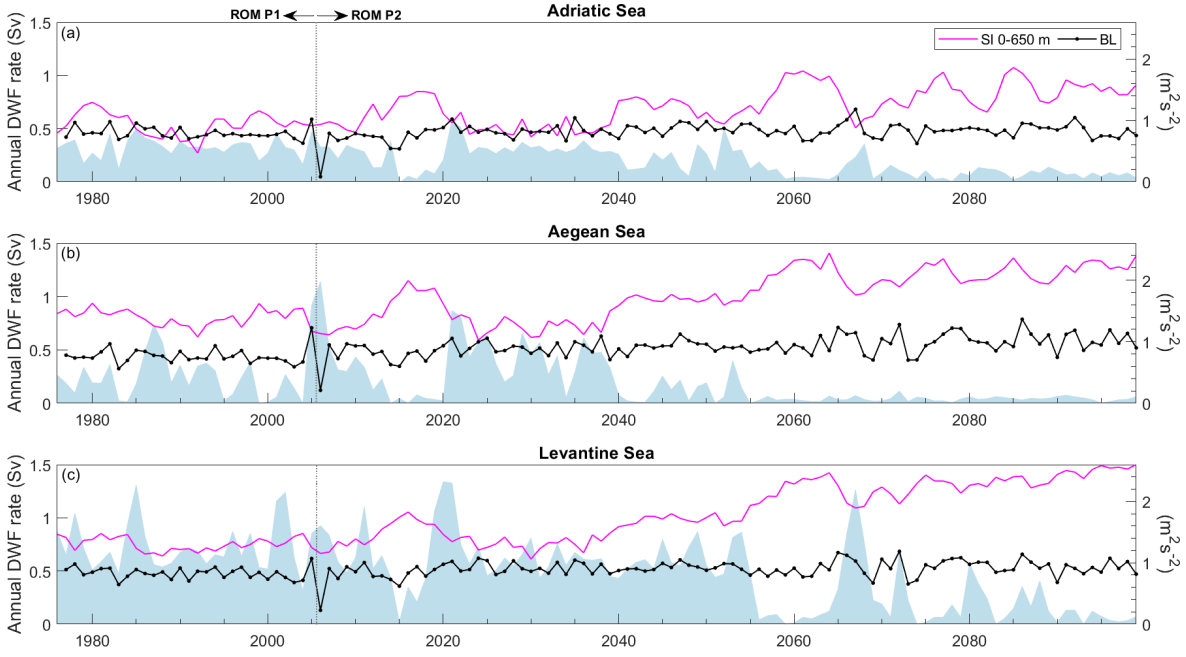

Figure 3. Time series (1976–2099) of ROM_P1 and ROM_P2 simulations of the yearly DWF rate (Sv) (filled area), winter integrated buoyancy loss (BL, $m^2\ s^{-2}$) (dotted black), and stratification index (SI, $m^2\ s^{-2}$) for 0–650 m (magenta) averaged over the **(a)** Adriatic Sea, **(b)** Aegean Sea, and **(c)** Levantine Sea. All time series correspond to winter months (December–January–February–March), whereas SI was computed in December of the preceding year.

1999; Somot et al., 2018; Parras-Berrocal et al., 2022):

$$\mathrm{BF} = g \cdot \left(\frac{\alpha \cdot Q_{\mathrm{net}}}{\rho_0 \cdot C_p} + \beta \cdot \mathrm{SSS} \cdot \mathrm{FWF} \right), \quad (1)$$

$$\mathrm{BL}(Y) = -\int_{T_1}^{T_2} \mathrm{BF} \cdot \mathrm{d}t, \quad (2)$$

where Q_{net} and FWF are the net surface heat and freshwater fluxes, respectively (both positive downward), g is the gravitational acceleration ($9.81\,\mathrm{m\,s^{-2}}$), α and β the thermal expansion and haline contraction coefficients (respectively calculated as a function of surface T and S), ρ_0 the reference density of seawater $1025\,\mathrm{kg\,m^{-3}}$, C_p the specific heat capacity of seawater (equal to $4000\,\mathrm{J\,kg^{-1}\,K^{-1}}$), and SSS the sea surface salinity.

To assess the pre-winter water column stratification we have computed the SI using December data. Low values of SI indicate a weak stratification in the water column. The SI is often used in Mediterranean studies (Somot et al., 2018; Margirier et al., 2020; Parras-Berrocal et al., 2022), and it is calculated following Turner (1973).

$$\mathrm{SI} = \int_0^h N^2 z \mathrm{d}z, \quad (3)$$

where N is the Brunt–Väisälä frequency ($N^2 = g/\rho_0 \partial_\rho / \partial_z$), z is the depth, ρ the potential density, and h the maximum depth of integration, which we have chosen to be 650 m because it is right below the LIW layer (150–600 m; Menna and Poulain, 2010).

Our results indicate that the intensity of the DWF rate is mostly determined by the SI (Pearson correlation coefficient $(r) > 0.7$ and p values are 0 in all regions), as a low or high amount of water produced can be found with similar BL values ($r < 0.1$ and p values > 0.05) (Fig. 3). For the 1976–2099 period the BL (SI) has a mean value of 0.81 ± 0.13 (1.17 ± 0.31), 0.89 ± 0.18 (1.68 ± 0.38), and $0.88 \pm 0.14\,\mathrm{m^2\,s^{-2}}$ ($1.73 \pm 0.46\,\mathrm{m^2\,s^{-2}}$) for the Adriatic, Aegean, and Levantine seas, in that order. Higher values of the DWF rate are linked to a low SI, which reflects a weaker stratification of the water column (Fig. 3a, b, and c). The BL does not show changes in the interannual variability in the trend. However, the Pettitt test indicates that from the 2040s the SI shows a change in the trend in the three regions (Table S1), which is especially remarkable in the Aegean and Levantine basins (Fig. 3b and c). From 2040, the SI steadily increases in the Adriatic ($5.43 \times 10^{-3}\,\mathrm{m^2\,s^{-2}\,yr^{-1}}$), showing a maximum of $1.86\,\mathrm{m^2 s^{-2}}$. The SI rises sharply in the Aegean ($9.59 \times 10^{-3}\,\mathrm{m^2\,s^{-2}\,yr^{-1}}$) and even more in the Levantine ($1.52 \times 10^{-2}\,\mathrm{m^2\,s^{-2}\,yr^{-1}}$), reaching values close to $2.5\,\mathrm{m^2\,s^{-2}}$ in both regions at the end of the 21st century. These changes strengthen the vertical stratification in the Adriatic, Aegean, and Levantine seas, hampering vertical mixing and thus deep convection.

The projected increase in SI comes from changes in the hydrographic characteristics of the water column. Under the RCP8.5 emission scenario the temperature and salinity are projected to increase through the whole water column in the main spots for dense water formation in the EMed (Fig. 4). By the end of the 21st century the Adriatic Sea will be warmer and saltier. The temperature in the upper ocean (0–100 m) will increase by 3.3 °C, while in the intermediate (100–600 m) and 600–1000 m layers it will increase by 2.6 and 2 °C (Fig. 4a). The salinity is expected to increase by 0.5 psu at 0–100 m and 0.4 psu at 100–600 and 600–1000 m (Fig. 4d). In the Adriatic, the warming and salinization are practically homogeneous from the surface to deep layers; however, in the Aegean and Levantine basins, the temperature and salinity increases start at the surface and are progressively transferred to deeper layers over the years (Fig. 4).

The Aegean Sea experiences a warming of 3.9 °C in the upper ocean. In the 100–600 m layer the temperature will increase by 2.7 °C, while in the deeper layer the warming is lower than 0.8 °C (Fig. 4b). The salinity in the upper layer is fresher than in deeper layers due to the net inflow of lighter water through the Dardanelles strait. It is precisely in this layer where the larger salinity increase is found (1 psu) by the end of the 21st century (Fig. 4e). The 100–600 and 600–1000 m layers also tend to get saltier by up to 0.6 and 0.2 psu, respectively. From the surface to intermediate depths the warming and salinization accelerate in the second half of the century.

The Levantine basin is where the higher EMed temperatures are found (Fig. 4c). The temperature is expected to increase, on average, by 3.6 °C in the 0–100 m layer. In the 100–600 and 600–1000 m layers the temperature will increase by 2.1 and 0.6 °C, which correspond to the lowest warming at those depths in comparison to the other spots for deep convection in the EMed. Finally, the salinity increases by 0.4 psu in the upper and intermediate layers and by 0.2 psu in the deeper layer by the end of the century (Fig. 4f). In the Aegean the projected increase in temperature and salinity also accelerates in the second half of the century.

To quantify the relative contribution of surface and intermediate water to the reduction in the intensity of DWF, we use the methodology applied in Parras-Berrocal et al. (2022). We compare the SI calculated from spatially and temporally averaged vertical profiles in the Adriatic, Aegean, and Levantine seas in four cases (Table 1 and Figs. S2, S3, and S4): (a) using the values corresponding to the historical period (1976–2005, Hist.), (b) using the last 30 years of RCP8.5 projection (2070–2099, Proj.), and also generating two synthetic profiles, (c) one including Hist. features for the first 100 m depth and Proj. characteristics for deeper layers (100–650 m depth), as well as (d) a second one using Proj. properties for the first 100 m depth and Hist. for deeper layers. In the Adriatic Sea, the results suggest that the change in AdSW characteristics causes 50 % of the total SI future change, while the contribution of LIW causes the other 50 %. In the Aegean

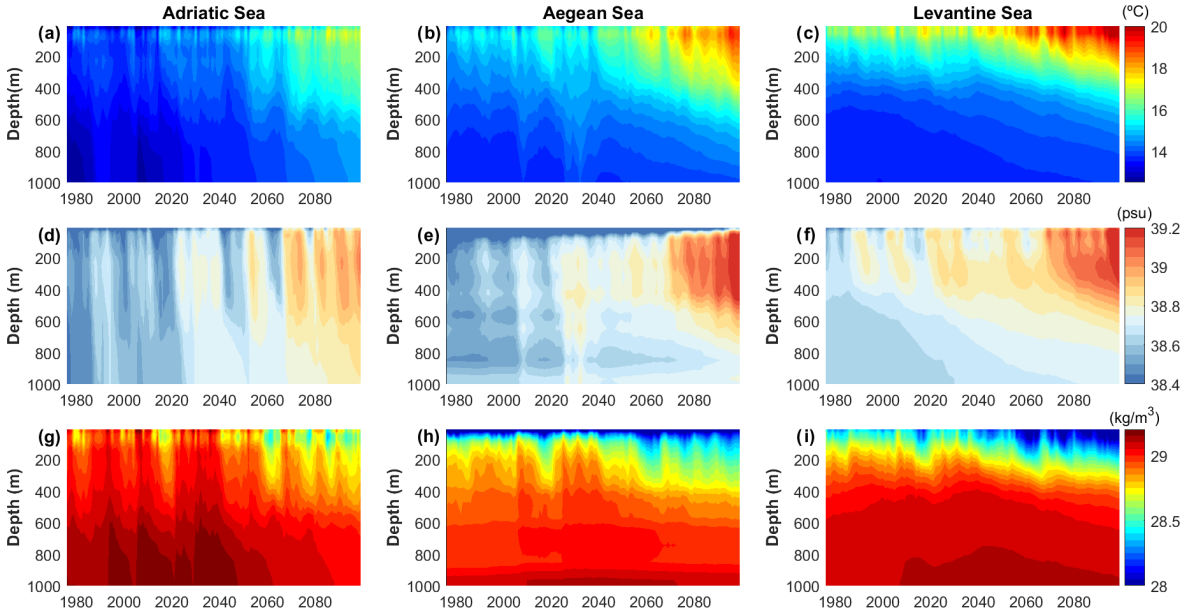

Figure 4. ROM RCP8.5 time series (1976–2099) of 0–1000 m **(a, b, c)** potential temperature (°C) as well as **(d, e, f)** salinity (psu) and **(g, h, i)** potential density (kg m^{-3}). All time series correspond to winter months (December–January–February–March) in the Adriatic **(a, d, g)**, Aegean **(b, e, h)**, and Levantine **(c, f, i)** seas.

Table 1. Stratification index (m^2 s^{-2}) and the quantification of the percentage of surface and intermediate water contributions calculated from vertical profiles presented in Figs. S2, S3, and S4.

	Adriatic Sea		Aegean Sea		Levantine Sea	
	SI	%	SI	%	SI	%
Hist. (1976–2005)	0.94	–	1.40	–	1.30	–
Proj. (2070–2099)	1.48	–	2.13	–	2.35	–
$(0–100\,m)_{Hist.} + (100–650\,m)_{Proj.}$	1.21	50.0 %	1.99	80.8 %	1.93	60.0 %
$(0–100\,m)_{Proj.} + (100–650\,m)_{Hist.}$	1.21	50.0 %	1.54	19.2 %	1.72	40.0 %

Sea, the alteration in BSW and LSW properties leads to 19.2 % of the total SI future change, while the change in CIW and LIW is 80.8 %. Finally, in the Levantine Sea changes in the AW and LSW properties contribute 40 %, whereas LIW contributes 60 %.

4 Discussion and conclusions

The impact of climate change on dense water formation in the EMed has briefly been assessed in previous studies (Somot et al., 2006; Adloff et al., 2015; Soto-Navarro et al., 2020). All authors considered the maximum of the winter mixed layer depth (MLD) to be a proxy for deep water convection. The results reported in those works do not show a consensus concerning the changes in the deep water formation role in the EMed. Somot et al. (2006) found that the maximum MLD decreases by about 20 % for the Aegean Sea and 60 % for the Levantine Sea in 2099 under the A2 scenario, whereas no significant change is expected for the Adriatic Sea. For this region, their simulations projected an increase in the DWF rate; however, the ADW outflowing through the Strait of Otranto is lighter, which leads to a weakening in the eastern Mediterranean thermohaline cell. The results obtained by Adloff et al. (2015) under the A2 scenario by the end of the 21st century point to the reduction of MLD in the Adriatic and Levantine seas, whereas it increases in the Aegean Sea. More recently, Soto-Navarro et al. (2020) found in a multi-model analysis that most models agree in projecting a reduction in the intensity of DWF in the Adriatic Sea by the end of the century under RCP4.5 and RCP8.5 scenarios. However, in the Aegean Sea the results are not robust among models, as some of them point to a reduction and others to an increase.

Due to the large spread in the simulated magnitude of the changes in the DWF in previous works (Somot et al., 2006; Adloff et al., 2015; Soto-Navarro et al., 2020), we try to identify the mechanisms involved in the expected changes in

the EMed DWF using a single model run: the same used in Parras-Berrocal et al. (2022) for identifying the mechanisms of the future change in DWF in the north-western Mediterranean. The projection was carried out with the RCSM ROM under the high-emission RCP8.5 scenario, and it was also a member (AWI25-MPI-8.5) of the ensemble used in Soto-Navarro et al. (2020). As in Parras-Berrocal et al. (2022), the drawback of using a single model run is that it does not allow us to provide robust conclusions and to generalize our results. However, the advantage of this approach is that it makes it easier to find physically consistent mechanisms responsible for these changes, making a valuable contribution to Med-CORDEX. Moreover, this kind of work provides essential information for future studies using multi-model ensemble analysis by deepening the processes. Indeed, the recent work of Josey and Schroeder (2023) highlights the importance of and the need for further research using climate models to understand the mechanisms involved in regional processes such as Mediterranean dense water formation and its consequences.

In this work we quantify deep water convection through the DWF rate. We estimate the annual DWF rate following the volume of deep water for a specific isopycnic surface (σ_θ), which is probably the most quantitative way to estimate the DWF, especially in model analysis (Somot et al., 2018). We show that ROM_P0 is capable of reproducing the average and interannual DWF rates in the main spots for deep convection in the EMed. Moreover, ROM_P0 captures the main features of the EMT (Roether et al., 1996), simulating higher DWF rates in the Aegean Sea than in the Adriatic Sea for winters from 1988 to 1994 (Fig. S5). In ROM_P0 the potential density of new deep water formed in the Adriatic ($\sigma > 29\,\mathrm{kg\,m^{-3}}$), Aegean ($\sigma > 28.95\,\mathrm{kg\,m^{-3}}$), and Levantine ($\sigma > 28.7\,\mathrm{kg\,m^{-3}}$) seas is lighter than the values presented in the literature (Lascaratos et al., 1993; Mantziafou and Lascaratos, 2008; Nittis et al., 2003). This could be explained by the negative salinity bias displayed throughout the entire water column (0–1000 m depth) by ROM_P0 over the EMed (Fig. S1). The largest salinity bias is found in the upper layers of the Aegean Sea (Fig. S1) as ROM_P0 overestimates the inflow of water through the Dardanelles strait, as previously reported by Parras-Berrocal et al. (2020). However, we are confident that this limitation does not impact our DWF study, as ROM_P0 has demonstrated a good representation of the deep water volume formed during the present climate, independently of the lower density values.

Our results project a DWF rate reduction of 75 % for the Adriatic Sea, 84 % for the Aegean Sea, and 83 % for the Levantine Sea by the end of the century under the RCP8.5 scenario. Analysing the mechanisms involved in the decrease, we observe that strong or weak DWF rates can occur with similar BL values (Fig. S6). We find out that changes in the hydrographic properties of the upper and intermediate water masses lead to a higher stratification of the water column in the Adriatic, Aegean, and Levantine basins, which hampers deep convection. Josey and Schroeder (2023) found using a multidecadal (1951–2020) observation-based analysis that the weakening heat loss is a potential factor in the reduction of dense water formation. The authors point to a possible dependence between the weakening heat loss and the stronger stratification which remains unexplored. Thus, it is essential for the Med-CORDEX community to clarify the relative contribution of both processes in forthcoming works.

In the future, temperature and salinity show an increase, which is especially noticeable in the 0–100 and 100–600 m layers. Those alterations in temperature and salinity will increase the vertical density gradient, which will in turn strengthen the stratification of the water column (Table 1). Recently, Amitai et al. (2021) found that a DWF decrease in the Adriatic Sea creates a state wherein warmer and saltier intermediate water reaching the north-western Mediterranean significantly affects the deep water convection in the Gulf of Lions. The reduction of EMed DWF as well as the DWF collapse expected in the north-western Mediterranean (Soto-Navarro et al., 2020; Parras-Berrocal et al., 2022) may have an impact on the deep ventilation and on the MTHC. Those changes are reflected in the flows exchanged between the Atlantic Ocean and the Mediterranean Sea through the Strait of Gibraltar (Parras-Berrocal et al., 2022).

As shown in Fig. 3, from 2020 to 2040 the DWF rate shows maxima in all DWF spots. During these 20 years, the SI shows minima due to an increase in potential density in the 0–100 m layer (Fig. S7). In the Adriatic Sea, changes in salinity are responsible for nearly all of the density change expected in the 2020–2040 period (Table S2). In the Aegean and Levantine seas, the salinity contribution to density changes (2020–2040) is 68.4 % and 63.6 %, respectively (Table S2). These results suggest that salinity changes are the only cause of those density changes in the Adriatic Sea and a primary factor in the Aegean and Levantine seas. In turn, such increased surface density preconditions the convective regions, reducing the vertical stratification and leading to the formation of larger volumes of deep water.

Another result worth discussing is that from 2005 to 2040 the annual DWF rate for the Aegean Sea is higher than for the Adriatic Sea in most of the years. For this period, the accumulated deep water in the Aegean Sea is 13.4 Sv yr, whereas in the Adriatic Sea it is 9.93 Sv yr. The results suggest a shift in the main source of EMDW from the Adriatic Sea to the Aegean Sea, as previously happened during the EMT. The HadCM2-SUL climate experiment (Thorpe and Bigg, 2000) has also shown a decrease in the intensity of deep convection in the Adriatic during 2040–2060, while it increases in the eastern basins. This is also supported by Adloff et al. (2015), who determined that the future MTHC tends to be similar to an EMT situation, with the Aegean Sea becoming the main source of EMDW in the future.

By the end of the century, in the Adriatic Sea a decrease in density of $0.1\,\mathrm{kg\,m^{-3}}$ is projected at a depth of 650 m with an average decrease over the entire water column of

0.2 kg m^{-3} (Figs. 4g and S8d). In contrast, in the Aegean Sea results do not show changes in density at 650 m depth, while the average decrease over the entire water column is 0.08 kg m^{-3} (Figs. 4h and S8e). In the Levantine Sea, we observe a reduction in density of 0.15 kg m^{-3} at both 300 m depth and throughout the entire water column (Figs. 4i and S8f). Based on the observed density reductions, we calculated the future changes in dense water formation rates in the Adriatic, Aegean, and Levantine seas (Fig. S9). In the Adriatic Sea, using a reference of 29 kg m^{-3}, a 75 % reduction in the DWF rate is projected. Using lower reference densities of 28.9 and 28.8 kg m^{-3} resulted in smaller reductions of 58 % and 39 %, respectively. In the Aegean Sea, where the density is expected to remain relatively stable, the sensitivity of the DWF rate to reference density values is negligible, with a projected decrease that varies from 84 % (using a density of 28.95 kg m^{-3}) to 80 % (using 29.9 kg m^{-3}). In the Levantine Sea, the reduction of the projected decrease in the DWF rate is more substantial, with a drop from 83 % (using a density of 28.7 kg m^{-3}) to 56 % (using 29.55 kg m^{-3}). Overall, the use of a lower isopycnal threshold leads to the same conclusions: a collapse of DWF in the Aegean Sea (Fig. S9b) and a notable reduction (of more than 50 %) in the Levantine basin (Fig. S9c). However, in the Adriatic Sea this is not the case, as the lowest isopycnal density threshold (28.8 kg m^{-3}, blue line in Fig. S9a) shows events with notable DWF rates during the last third of the century.

We noted different DWF rate responses to changes in density threshold for each sub-basin. In the Adriatic Sea, the future changes in DWF strongly depend on the density change in the water column and therefore on the choice of the density threshold, with denser isopycnals corresponding to stronger DWF rate reductions and no remarkable DWF change for the less dense threshold (Fig. S9d). In the Aegean Sea, a collapse of DWF is expected regardless of the density reference used. Finally, in the Levantine Sea, the changes in the DWF rate appear to have a limited dependence on the choice of the density threshold. The reduction in the DWF rate is 83 % for 28.7 kg m^{-3} and 56 % for 28.55 kg m^{-3}, so the reduction is noticeable in both cases, although it is sensitive to the choice of the density threshold.

Data availability. The model data are available online (https://doi.org/10.5281/zenodo.7594313, Parras-Berrocal et al., 2023).

Supplement. The supplement related to this article is available online at: https://doi.org/10.5194/os-19-941-2023-supplement.

Author contributions. IMPB, AI, and WC planned the study. AI and IMPB designed the analysis framework. IMPB processed data, conducted the analysis, and wrote the paper. DVS performed the ROM runs. RV, WC, DVS, OA, MB, and AI contributed with the analysis performance and interpretation of the results. AI revised and edited the final version of the paper. IMPB prepared everything.

Competing interests. The contact author has declared that none of the authors has any competing interests.

Disclaimer. Publisher's note: Copernicus Publications remains neutral with regard to jurisdictional claims in published maps and institutional affiliations.

Acknowledgements. Simulations were done at the German Climate Computing Center (DKRZ). This work is part of the MedCORDEX (https://www.medcordex.eu, last access: 19 January 2023) initiative and the HyMex programme (https://www.hymex.org, last access: 19 January 2023).

Financial support. Iván M. Parras-Berrocal was supported by the Spanish National Plan for Scientific and Technical Research and Innovation through project TRUCO (RTI2018-100865-B-C22) and the Plan Propio UCA 2022-23. Rubén Vázquez has been funded by the Spanish Ministry of Science, Innovation and Universities through grant PID2021-128656OB-I00. William Cabos has been supported by Alcala University (project PIUAH21/CC-058) and the Spanish Ministry of Science, Innovation and Universities through grant PID2021-128656OB-I00. Dimitry V. Sein received funding from the Federal Ministry of Education and Research of Germany (BMBF) in the framework of ACE (grant no. 01LP2004A) and the Ministry of Science and Higher Education of Russia (theme no. FMWE-2021-0014). Publisher's note: the article processing charges for this publication were not paid by a Russian or Belarusian institution.

Review statement. This paper was edited by Xinping Hu and reviewed by two anonymous referees.

References

Adloff, F., Somot, S., Sevault, F., Jordà, G., Aznar, R., Déqué, M., Herrmann, M., Marcos, M., Dubois, C., Padorno, E., and Alvarez-Fanjul, E.: Mediterranean Sea response to climate change in an ensemble of twenty first century scenarios, Clim. Dynam., 45, 2775–2802, https://doi.org/10.1007/s00382-015-2507-3, 2015.

Ali, E., Cramer, W., Carnicer, J., Georgopoulou, E., Hilmi, N. J. M., Le Cozannet, G., and Lionello, P.: Cross-Chapter Paper 4: Mediterranean Region, in: Climate Change 2022: Impacts, Adaptation and Vulnerability. Contribution of Working Group II to the Sixth Assessment Report of the Intergovernmental Panel on Climate Change, edited by: Pörtner, H.-O., Roberts, D. C., Tignor, M., Poloczanska, E. S., Mintenbeck, K., Alegría, A., Craig, M., Langsdorf, S., Löschke, S., Möller, V., Okem, A., and Rama, B.,

Cambridge University Press, Cambridge, UK and New York, NY, USA, 2233–2272, 2022.

Amitai, Y., Ashkenazy, Y., and Gildor, H.: The Effect of the Source of Deep Water in the Eastern Mediterranean on Western Mediterranean Intermediate and Deep Water, Front. Mar. Sci., 7, 615975, https://doi.org/10.3389/fmars.2020.615975, 2021.

Androulidakis, Y., Kourafalou, V. H., Krestenitis, Y. N., and Zervakis, V.: Variability of deep water mass characteristics in the North Aegean Sea: the role of lateral inputs and atmospheric conditions, Deep-Sea Res. Pt. I, 67, 55–72, https://doi.org/10.1016/j.dsr.2012.05.004, 2012.

Béthoux, J. P. and Gentili, B.: Functioning of the Mediterranean Sea: past and present changes related to freshwater input and climate changes, J. Marine Syst., 20, 33–47, https://doi.org/10.1016/S0924-7963(98)00069-4, 1999.

Beuvier, J., Sevault, F., Herrmann M., Kontoyiannis, H., Ludwig, W., Rixen, M., Stanev, E., Beranger, K., and Somot, S.: Modeling the Mediterranean Sea interannual variability during 1961–2000: Focus on the Eastern Mediterranean Transient, J. Geophys. Res., 115, C08017, https://doi.org/10.1029/2009JC005950, 2010.

Borzelli, G. L. E., Gacic, M., Cardin, V., and Civitarese, G.: Eastern Mediterranean Transient and reversal of the Ionian Sea circulation, Geophys. Res. Lett., 36, L15108, https://doi.org/10.1029/2009GL039261, 2009.

Boyer, T. P., Garcia, H. E., Locarnini, R. A., Zweng, M. M., Mishonov, A. V., Reagan, J. R., Weathers, K. A., Baranova, O. K., Seidov, D., and Smolyar, I. V.: World Ocean Atlas 2018, NOAA National Centers for Environmental Information [data set], https://www.ncei.noaa.gov/archive/accession/NCEI-WOA18 (last access: 6 March 2023), 2018.

Darmaraki, S., Somot, S., Sevault, F., Nabat, P., Cabos Narvaez, W. D., Cavicchia, L., Djurdjevic, V., Li, L., Sannino, G., and Sein, D. V.: Future evolution of Marine Heatwaves in the Mediterranean Sea, Clim. Dynam., 53, 1371–1392, https://doi.org/10.1007/s00382-019-04661-z, 2019.

de la Vara, A., Parras-Berrocal, I. M., Izquierdo, A., Sein, D. V., and Cabos, W.: Climate change signal in the ocean circulation of the Tyrrhenian Sea, Earth Syst. Dynam., 13, 303–319, https://doi.org/10.5194/esd-13-303-2022, 2022.

Dunic, N., Vilibic, I., Sepic, J., Somot, S., and Sevault, F.: Dense water formation and BiOS-induced variability in the Adriatic simulated using an ocean regional circulation model, Clim. Dynam., 51, 1211–1236, https://doi.org/10.1007/s00382-016-3310-5, 2018.

Gačić, M., Civitarese, G., Miserocchi, S., Cardin, V., Crise, A., and Mauri, E.: The open-ocean convection in the Southern Adriatic: a controlling mechanism of the spring phytoplankton bloom, Cont. Shelf Res., 22, 1897–1908, https://doi.org/10.1016/S0278-4343(02)00050-X, 2002.

Hagemann, S. and Dümenil-Gates, L.: A parameterization of the lateral waterflow for the global scale, Clim. Dynam., 14, 17–31, https://doi.org/10.1007/s003820050205, 1998.

Hagemann, S. and Dümenil-Gates, L.: Validation of the hydrological cycle of ECMWF and NCEP reanalysis using the MPI hydrological discharge model, J. Geophys. Res., 106, 1503–1510, https://doi.org/10.1029/2000JD900568, 2001.

Hibler, W. D.: A dynamic thermodynamic sea ice model, J. Phys. Oceanogr., 9, 815–846, https://doi.org/10.1175/1520-0485(1979)009<0815:ADTSIM>2.0.CO;2, 1979.

Incarbona, A., Martrat, B., Mortyn, P.G., Sprovieri, M., Ziveri, P., Gogou, A., Jordà, G., Xoplaki, E., Luterbacher, J., Langone, L., Marino, G., Rodríguez-Sanz, L., Triantaphyllou, M., Di Stefano, E., Grimalt, J.-O., Tranchida, G., Sprovieri, R., and Mazzola, S.: Mediterranean circulation perturbations over the last five centuries: Relevance to past Eastern Mediterranean transient-type events, Sci. Rep.-UK, 6, 1–10, https://doi.org/10.1038/srep29623, 2016.

Jacob, D.: A note to the simulation of the annual and interannual variability of the water budget over the Baltic Sea drainage basin, Meteorol. Atmos. Phys., 77, 61–73, https://doi.org/10.1007/s007030170017, 2001.

Jungclaus, J. H., Fischer, N., Haak, H., Lohmann, K., Marotzke, J., Matei, D., Mikolajewicz, U., Notz, D., and von Storch, J. S.: Characteristics of the ocean simulations in MPIOM, the ocean component of the MPI-Earth system model, J. Adv Model. Earth Sy., 5, 422–446, https://doi.org/10.1002/jame.20023, 2013

Klein, B., Roether, W., Manca, B. B., Bregant, D., Beitzel, V., Kovacecic, V., and Lucchetta, A.: The large deep water transient in the Eastern Mediterranean, Deep-Sea Res. Pt. I, 46, 371–414, https://doi.org/10.1016/S0967-0637(98)00075-2, 1999.

Klein, B., Roether, W., Civitarese, G., Gacic, M., Manca, B. B., and d'Alcala, M. A.: Is the Adriatic returning to dominate the production of Eastern Mediterranean deep water?, Geophys. Res. Lett., 27, 3377–3380, https://doi.org/10.1029/2000GL011620, 2000.

Lascaratos, A., Williams, R., and Tragou, E.: A mixed-layer study of the formation of Levantine Intermediate Water, J. Geophys. Res., 98, 14739–14749, https://doi.org/10.1029/93JC00912, 1993.

Lascaratos, A., Roether, W., Nittis, K., and Klein, B.: Recent changes in deep water formation and spreading in the eastern Mediterranean Sea: a review, Prog. Oceanogr., 44, 5–36, https://doi.org/10.1016/S0079-6611(99)00019-1, 1999.

Levitus, S., Boyer, T. P., Conkright, M. E., O'Brien, T., Antonov, J., Stephens, C., Stathoplos, L., Johnson, D., and Gelfeld, R.: World Ocean Database 1998, Vol. 1, Introduction, NOAA Atlas NESDIS 18, Ocean Clim. Lab., Natl. Oceanogr. Data Cent., U.S. Gov. Print. Off., Washington, D.C., https://repository.library.noaa.gov/view/noaa/49345/noaa_49345_DS1.pdf (last access: 23 June 2023), 1998.

Li, P. and Tanhua, T.: Recent changes in deep ventilation of the Mediterranean Sea; Evidence from long-term transient tracer observations, Front. Mar. Sci., 7, 594, https://doi.org/10.3389/fmars.2020.00594, 2020.

Maier-Reimer, E., Kriest, I., Segschneider, J., and Wetzel, P.: The HAMburg Ocean Carbon Cycle Model HAMOCC5.1 Technical Description Release 1.1, Ber. Erdsystemforschung, 14, http://hdl.handle.net/11858/00-001M-0000-0011-FF5C-D (last access: 30 January 2023), 2005.

Malanotte-Rizzoli, P., Manca, B. B., D'Alcalà, M. R., Theocharis, A., Bergamasco, A., Bregant, D., Budillon, G., Civitarese, G., Georgopoulos, D., Michelato, A., Sansone, E., Scarazzato, P., and Souvermezoglou, E.: A synthesis of the Ionian Sea hydrography, circulation, and water mass pathways during POEM-Phase I, Prog. Oceanogr., 39, 153–204, https://doi.org/10.1016/S0079-6611(97)00013-X, 1997.

Manca, B., Kovacevic, V., Gacic, M., and Viezzoli, D.: Dense water formation in the Southern Adriatic Sea and spreading into the

Ionian Sea in the period 1997–1999, J. Marine Syst., 33–34, 133–154, https://doi.org/10.1016/S0924-7963(02)00056-8, 2002.

Mantziafou, A. and Lascaratos, A.: Deep-water formation in the Adriatic Sea: Interannual simulations for the years 1979–1999, Deep-Sea Res. Pt. I, 55, 1403–1427, https://doi.org/10.1016/j.dsr.2008.06.005, 2008.

Margirier, F., Testor, P., Heslop, E., Mallil, K., Bosse, A., Houpert, L., Mortier, L., Bouin, M.-B., Coppola, L., D'Ortenzio, F., Durrie de Madron, X., Mourre, B., Prieur, L., Raimbault, P., and Taillandier, V.: Abrupt warming and salinification of intermediate waters interplays with decline of deep convection in the Northwestern Mediterranean Sea, Sci. Rep.-UK, 10, 20923, https://doi.org/10.1038/s41598-020-77859-5, 2020.

Marshall, J. and Schott, F.: Open-ocean convection: observations, theory, and models, Rev. Geophys., 37, 1–64, https://doi.org/10.1029/98RG02739, 1999.

Marsland, S. J., Haak, H., Jungclaus, J. H., Latif, M., and Roeske, F.: The Max-Planck- Institute global ocean/sea ice model with orthogonal curvilinear coordinates, Ocean Model., 5, 91–127, https://doi.org/10.1016/S1463-5003(02)00015-X, 2003.

MEDOC Group: Observations of formation of deep-water in the Mediterranean Sea, Nature, 227, 1037–1040, https://doi.org/10.1038/2271037a0, 1970.

Menna, M. and Poulain, P. M.: Mediterranean intermediate circulation estimated from Argo data in 2003–2010, Ocean Sci., 6, 331–343, https://doi.org/10.5194/os-6-331-2010, 2010.

Millot, C.: Levantine Intermediate Water characteristics: an astounding general misunderstanding! (addendum), Sci. Mar., 78, 165–171, https://doi.org/10.3989/scimar.04045.30H, 2014.

Millot, C.: Comments about computations about the Mediterranean Outflow composition, B. Geofis. Teor. Appl., 60, 517–630, https://doi.org/10.4430/bgta0266, 2019.

Nittis, K., Lascaratos, A., and Thocharis, A.: Dense water formation in the Aegean Sea: Numerical simulations during the Eastern Mediterranean Transient, J. Geophys. Res., 108, 8120, https://doi.org/10.1029/2002JC001352, 2003.

Ovchinnikov, I. M.: The formation of intermediate water in the Mediterranean, Oceanology, 24, 168–173, 1984.

Parras-Berrocal, I. M., Vazquez, R., Cabos, W., Sein, D., Mañanes, R., Perez-Sanz, J., and Izquierdo, A.: The climate change signal in the Mediterranean Sea in a regionally coupled atmosphere–ocean model, Ocean Sci., 16, 743–765, https://doi.org/10.5194/os-16-743-2020, 2020.

Parras-Berrocal, I. M., Vazquez, R., Cabos, W., Sein, D., Álvarez, O., Bruno, M., and Izquierdo, A.: Surface and Intermediate Water Changes Triggering the Future Collapse of Deep Water Formation in the North Western Mediterranean, Geophys. Res. Lett., 49, e2021GL095404, https://doi.org/10.1029/2021GL095404, 2022.

Parras-Berrocal, I. M., Vazquez, R., Cabos, W., Sein, D., Alvarez, O., Bruno, M., and Izquierdo, A.: ROM model data for Eastern Mediterranean Dense Water Formation, Zenodo [data set], https://doi.org/10.5281/zenodo.7594313, 2023.

Pettitt, A. N.: A non-parametric approach to change-point problem, Appl. Statist., 28, 126–135, https://doi.org/10.2307/2346729, 1979.

Pollack, M., J.: The sources of the deep water of the eastern Mediterranean Sea, J. Mar. Res., 10, 128–152, 1951.

Rechid, D. and Jacob, D.: Influence of monthly varying vegetation on the simulated climate in Europe, Meteorol. Z., 15, 99–116, https://doi.org/10.1127/0941-2948/2006/0091, 2006.

Roether, W. and Schlitzer. R.: Eastern Mediterranean deep water renewal on the basis of chloro-fluoromethane and tritium data, Dynam. Atmos. Oceans, 15, 333–354, https://doi.org/10.1016/0377-0265(91)90025-B, 1991.

Roether, W., Manca, B. B., Klein, B., Bregant, D., Georgopoulos, D., Beitzel, V., Kovacevic, V., and Luchetta, A.: Recent changes in eastern Mediterranean deep waters, Science, 271, 333–335, https://doi.org/10.1126/science.271.5247.333, 1996.

Roether, W., Klein, B., and Hainbucher, D.: The Eastern Mediterranean Transient: evidence for similar evens previously?, in: The Mediterranean Sea: Temporal Variability and Spatial Patterns, Geophysical Monograph 202, edited by: Eusebi Borzelli, G. L., Gacić, M., Lionello, P., and Malanotte-Rizzoli, P., American Geophysical Union, John Wiley & Sons, Inc, 75–83, https://doi.org/10.1002/9781118847572.ch6, 2014.

Sánchez-Gómez, E., Somot, S., Josey, S. A., Dubois, C., Elguindi, N., and Déqué, M.: Evaluation of Mediterranean Sea water and heat budgets simulated by an ensemble of high resolution regional climate models, Clim. Dynam., 37, 2067–2086, https://doi.org/10.1007/s00382-011-1012-6, 2011.

Schlitzer, R., Roether, W., Oster, H., Junghans, H., Hausmann, M., Johannsen, H., and Michelato, A.: Chlorofluoromenthane and oxygen in the eastern Mediterranean, Deep-Sea Res. Pt. A, 38, 1531–1551, https://doi.org/10.1016/0198-0149(91)90088-W, 1991.

Sein, D. V., Mikolajewicz, U., Gröger, M., Fast, I., Cabos, W., Pinto, J. G., Hagemann, S., Semmler, T., Izquierdo, A., and Jacob, D.: Regionally coupled atmosphere-ocean-sea ice-marine biogeochemistry model ROM: 1. Description and validation, J. Adv. Model. Earth Sy., 7, 268–304, https://doi.org/10.1002/2014MS000357, 2015.

Josey, S. and Schroeder, K.: Declining winter heat loss threatens continuing ocean convection at a Mediterranean dense water formation site, Environ. Res. Lett., 18, 024005, https://doi.org/10.1088/1748-9326/aca9e4, 2023.

Somot, S., Sevault, F., and Déqué, M.: Transient climate change scenario simulation of the Mediterranean Sea for the 21st century using a high-resolution ocean circulation model, Clim. Dynam., 27, 851–879, https://doi.org/10.1007/s00382-006-0167-z, 2006.

Somot, S., Sevault, F., Déqué, M., and Crépon, M.: 21st century climate change scenario for the Mediterranean using a coupled atmosphere-ocean regional climate model, Global Planet. Change, 63, 112–126, https://doi.org/10.1016/j.gloplacha.2007.10.003, 2008.

Somot, S., Houpert, L., Sevault, F., Testor, P., Bosse, A., Taupier-Letage, I., Bouin, M. N., Waldman, R., Cassou, C., Sanchez-Gomez, E., Durrieu de Madron, X., Adloff, F., Nabat, P., and Herrman, M.: Characterizing, modelling and understanding the climate variability of the deep water formation in the North-Western Mediterranean Sea, Clim. Dynam., 51, 1179–1210, https://doi.org/10.1007/s00382-016-3295-0, 2018.

Soto-Navarro, J., Jordá, G., Amores, A., Cabos, W., Somot, S., Sevault, F., Macias, D., Djurdjevic, V., Sannino, G., Li, L., and Sein, D.: Evolution of Mediterranean Sea water properties under climate change scenarios in the Med-CORDEX ensemble,

Clim. Dynam., 54, 2135–2165, https://doi.org/10.1007/s00382-019-05105-4, 2020.

The LIWEX Group: The Levantine Intermediate Water Experiment (LIWEX) Group: Levantine Basin a laboratory for multiple water mass formation processes, J. Geophys. Res., 108, 8101, https://doi.org/10.1029/2002JC001643, 2003.

Thorpe, R. B. and Bigg, G. R.: Modelling the sensitivity of Mediterranean Outflow to anthropogenically forced climate change, Clim. Dynam., 16, 355–368, https://doi.org/10.1007/s003820050333, 2000.

Turner, J.: Buoyancy effects in fluids: Cambridge monographs on mechanics and applied mathematics, Cambridge University Press, Cambridge, https://doi.org/10.1017/CBO9780511608827, 1973.

Tziperman, E. and Speer, K.: A study of water mass transformation in the Mediterranean Sea: Analysis of climatological data and a simple 3-box model, Dynam. Atmos. Oceans, 21, 53–82, https://doi.org/10.1016/0377-0265(94)90004-3, 1994.

Valcke, S.: The OASIS3 coupler: a European climate modelling community software, Geosci. Model Dev., 6, 373–388, https://doi.org/10.5194/gmd-6-373-2013, 2013.

Vazquez, R., Parras-Berrocal, I., Cabos, W., Sein, D. V., Mañanes, R., and Izquierdo, A.: Assessment of the Canary current upwelling system in a regionally coupled climate model, Clim. Dynam., 58, 69–85, https://doi.org/10.1007/s00382-021-05890-x, 2022.